

# A Study on the Structural and Formation of the Low-Level Jet Stream over the Northern Persian Gulf (Case study on sinking the Behbahan cargo vessel)

Mehri Hashemi Devin<sup>1</sup>, Abbas Ranjbar\*<sup>2</sup>, Ebrahim Fattahi<sup>2</sup>, Sara Karami<sup>3</sup>, Saviz Sehat Kashani<sup>3</sup>

<sup>1</sup> PhD student, Atmospheric Science and Meteorological Research Center (ASMERC), Tehran, Iran

<sup>2</sup>\* Associate Prof. of Atmospheric Science and Meteorological Research (ASMERC), Tehran, Iran;  
[aranjbar@gmail.com](mailto:aranjbar@gmail.com)

<sup>3</sup> Assistant Professor, Atmospheric Science and Meteorological Research Center (ASMERC), Tehran, Iran

## ARTICLE INFO

### Article History:

Received: 04 Nov. 2020

Accepted: 09 Dec. 2020

### Keywords:

Low Level Jet

Persian Gulf

speed

Behbahan cargo vessel

WRF-ARW model

wind vertical profile

## ABSTRACT

A strong low level jet (LLJ) in the northern region of the Persian Gulf (PG) observed on 5th Jun 2020 that sank the Behbahan cargo vessel. In this article, we have used the WRF-V3 model and reanalysis ERA5 data to study the vertical structure, diurnal variation and intensity of the LLJs. The aimed topography's region, the pressure gradient and the land-sea breeze are the essential key factors in analyzing the diurnal variation of the LLJ over the PG that is known as the Shamal wind. The low terrain height in the northern of the PG and Zagros Mountains channelized the northwest winds and increased the pressure gradient that increased the wind speed. The decreasing friction over the PG during nighttime and the differences in temperature and specific heat capacity between water and land cause an increase in the LLJ intensity. The LLJ's core 22-24 ms<sup>-1</sup> was located over the study region in 925hPa on 4th and 5th June at 18 and 00 UTC respectively. Thereafter core's wind speed decreased to 10-14 ms<sup>-1</sup> at 12UTC on 5th June. The mix-down of momentum from the LLJ level to the surface caused an increase in wind speed and wave height over the PG which sank the Behbahan cargo vessel at early morning of 5th June. The LLJ at some regions like Kuwait formed at lower heights (under 950 hPa) and at the other points LLJ formed at levels upper than 950 hPa during nighttime of 4th Jun to afternoon of 5th Jun.

## 1. Introduction

Low Level Jet Stream (LLJ) is a very strong flow at levels near the surface (in boundary layer) with strong vertical wind shear ( $\partial \vec{V} / \partial z$ ) above and below of the core by wind speed more than 10 ms<sup>-1</sup>. Some LLJs result from strong baroclinity like fronts and some others are from any specific synoptic system with a weak baroclinity. The LLJ's importance and its effects on turbulence, wind energy production, distribution of pollutants and dust, aviation safety, increasing the height of waves on the sea and ocean have studied (Bonner, 1968; Doyle and Warner., 1993; Whiteman et al., 1997; Colle and Novak., 2010; Rife et al., 2010; Hu et al., 2013; Berg et al., 2015; Vanderwende et al., 2015; Smith et al., 2019). Several mechanisms proposed to describe the occurrence and characteristics of LLJs in some parts of the world in previous studies. The first theory was proposed by Blackadar (1957),

who addressed LLJs which result from an inertial oscillation, and their importance for the development of nighttime inversions. A second theory was developed by Holton (1967), who noted that the development of diurnal wind variations due to the diurnal heating and cooling of sloping terrain could affect the LLJs' intensity, a theory that was later examined and discussed by Bonner and Paegle (1970). By cooling the surface during nighttime, turbulent mixing stops, and the friction of the surface layer decreases significantly, so the middle and upper layer decouples from the surface. The balance between pressure gradient force and Coriolis force disrupts and this imbalance cause an inertial oscillation in wind and changes the geostrophic balance to super geostrophic wind and also increased wind speed at low level during nighttime (Markowski and Richardson., 2010). LLJ is primarily a thermal phenomenon and reaches heights where the vertical temperature profile forms an

inversion (e.g. Membery, 1983; Rao et al., 2003). Surface winds are mostly weaker or calm during night but upper winds could accelerate to LLJ or nighttime jet that increase to super geostrophic wind speed (Stull, 1988). LLJ over complex terrain in south of Iran is simulated (Liu et al, 2000). The result of the study about LLJ northerly jet on 12-14 Feb 1995 showed that this LLJ mobilized and transported dust from Lut desert to Oman Gulf and decreased visibility. Because of lack of the data and synoptic stations the WRF model is used to simulate the vertical cross section to study the wind of 120 days and dust storm activity over the Sistan basin (Alizadeh et al, 2014). The simulated jet cores in Yerevan are mostly located between 150 and 250 above ground with magnitudes varying from 12 to 21  $\text{ms}^{-1}$  (Gevorgyan, 2018). The climatology of the LLJ in Dashte Kavir is studied by using ERA-I reanalysis data during 1979-2017 that the core of jet has been identified at 850 hpa (Vazifeh et al, 2018). There is a strong correlation between northerly wind and meridional pressure gradient in Lut desert which are the important factors. Cold air advection from high latitude and also pressure gradient are important to form the gap wind (Bidokhti et al, 2006). Mobarak.H and Gaffarian (2018) simulated the LLJ by using different boundary layer schemes in WRF-CHEM model and LLJ's effect on the Khuzestan local dust studied. They concluded that LLJ has a key role on dust emission over semi-arid and arid area. Results from some studies (Membery, 1983; Giannakopoulou, 2012) show that LLJs cross of the northern region of the PG that cause strong wind speed over the PG and its ports and also increase the height of the waves so detection LLJ, its intensity and the LLJ structure in our study region are very important. On Friday morning 05 Jun 2020, the strong wind speed over water of the north of the PG near to Iraq, Um-Qasr port, drown the Behbahan vessel with seven person (Fig.1). In this paper, the strong wind over the Persian Gulf and the role of LLJ would be studied.

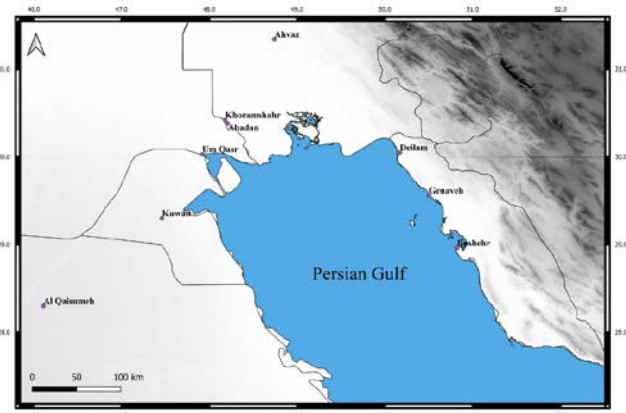


Figure 1. Topography map of the study area (PG)

## 2. Materials and methods

### 2.1. Study area

The northern of the PG is near-complex terrain with high and steep mountains, including the Zagros Mountains in Iran to the east (Fig.1), Kuwait in the west, and Khuzestan province in the north. Over the PG's complex terrain, diurnal mountain winds are generated by horizontal pressure differences that develop daily over the heated and cooled sloping terrain. It is thus apparent that the land-sea distribution (strong north-to-south pressure gradient) enhances the geostrophic wind speed that is vital factor. Boundary layer jets (BLJs), which are one type of low level jet, frequently occur next to a large mountain range or in regions with land-sea thermal contrast (Rife et al, 2010; Du et al, 2015).

### 2.2. Materials

Synoptic stations data (temperature, humidity, wind direction, wind speed, etc.) of Khuzestan and Bushehr provinces and Kuwait station data from 3th to 6th Jun 2020 extracted from MCI<sup>1</sup> system. Ahvaz and Al-Qaisumah (the nearest stations to Um Qasr, a port city in southern Iraq) upper air sounding data are used to study instability indexes and wind shear from surface to upper. Kuwait didn't record upper data on 3th to 6th Jun 2020. Because of lack of upper air data and the importance of the study of upper wind to distinguish LLJ in the PG region, we have used the output data of the model to show vertical profile of wind in the study region. The model used for this LLJ event is the WRF (ARW) model, version 3.9. The model performed from 3th to 6th Jun 2020. The 37 sigma levels employed within 1000 to 100hPa. Two-step nesting (one-way) was applied using two model domains centered at 9 and 27 km spatial resolutions (Fig.2).

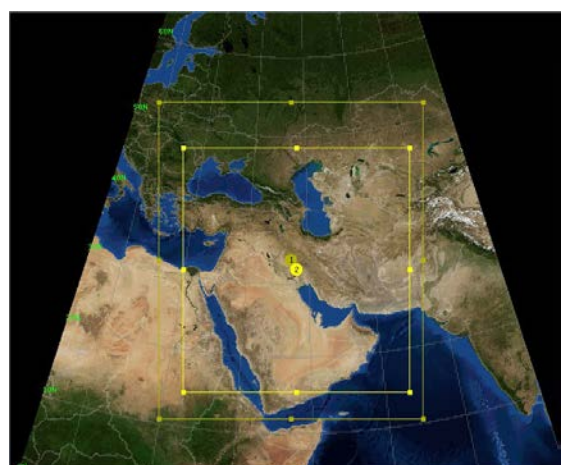


Figure 2. The WRF model domains with 9 and 27 km spatial resolutions (yellow dot indicates the centers of both domains located over the PG)

The selected schemes are widely used within the WRF community and have been shown to perform well over different regions. Like the unified Noah land-surface

<sup>1</sup> Meteorological Communication & Information

model scheme (Chen and Dudhia 2001), other physics was kept constant in the simulation. The WRF Single-Moment 3-Class Microphysics scheme (WSM3), Dudhia shortwave radiation scheme (Dudhia, 1989), Rapid Radiative Transfer Model (RRTM) longwave radiation scheme (Mlawer et al., 1997) have been selected. Mean sea level pressure, geopotential heights and wind fields in different levels were used from the model data and ERA5 data to study wind speed over our study region (PG and Um Qasr). To better identification the place of formation LLJ, some cross section of wind speed and potential temperature used. To identify the intensity and time of the LLJ formation vertical cross section of wind used.

### 3. Results and Discussion

#### 3.1 Synoptic pressure patterns associated with LLJ

Figure 3 shows the surface pressure map and 10-m wind on 4-5 Jun 2020. The surface pressure pattern shows a low pressure system over the PG that its trough extends to the Khuzestan which form a north and northwesterly wind over the PG and Khuzestan. A upper-latitude thermal high system over the Zagros Mountains increased the lower pressure gradient over east and southeast of Khuzestan and increased the lower troposphere wind speed over northwest of Bushehr on 4th Jun 2020 morning (00UTC) (Fig3.a).

On 4th Jun at 12UTC, the maximum wind is located over north of Bushehr and northeast of the PG.

There is a high pressure system over west of Iraq that extends to the west of Iran. The high pressure system

over the Zagros Mountains is stationary that cause a pressure gradient over Bushehr and Khuzestan (Fig.3, a, b). At 00 UTC on 5th Jun a low pressure system intensified as its central pressure reached less than 1004hPa and elongated to high latitudes where it was located over northeast of the PG and some parts of Bushehr. This pressure pattern would cause a northern and northwesterly winds (Fig.3.c).

The maximum 10-m wind speed is located over north of the PG and the wind speed over all northern parts of PG increased to  $16 \text{ ms}^{-1}$  during morning on 5th Jun. During 5th Jun's afternoon the pressure trough gradually extends to high latitudes over Khuzestan that caused the pressure gradient to decrease in the study area so the wind speed increased over Khuzestan and PG (Fig.3.d).

During afternoon time (12UTC) on 4th Jun at 925hPa level northerly wind speed increased sharply to  $20 \text{ ms}^{-1}$  over most of the PG (Fig.4.a). There is a low pressure system over south of the PG and an upper high over most of Iraq area that causes northerly wind over southwest of Iran (Fig.4.a, b). On the night of 04th Jun (18UTC) the wind speed increased sharply to  $26 \text{ ms}^{-1}$  and the maximum of wind was located over north of the PG and northwest of Bushehr (Fig.4.c). During local early morning time on 05 Jun (00UTC) the maximum wind speed extended to a more extensive area and during afternoon time the wind speed decreased (Fig.4.d). Figure 5.a, b present the 850 hPa geopotential height and wind speed that are northerly over the study region and during evening local time (12, 18 UTC) the wind speed increased from  $14 \text{ ms}^{-1}$  to  $20 \text{ ms}^{-1}$ .

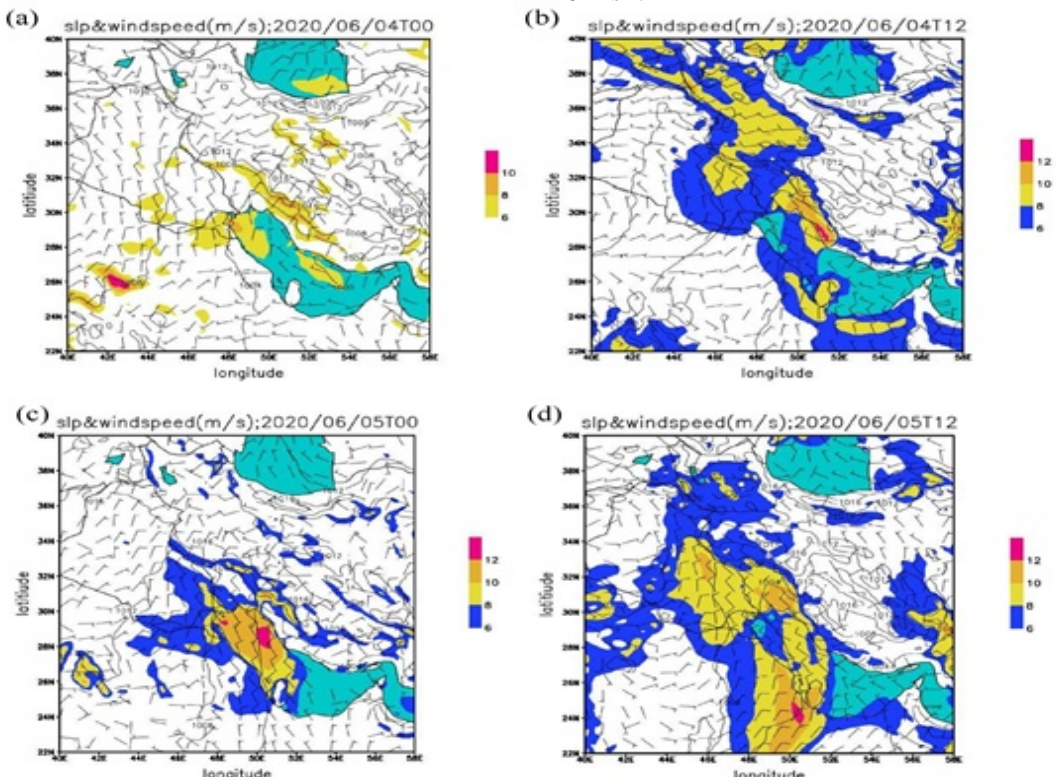
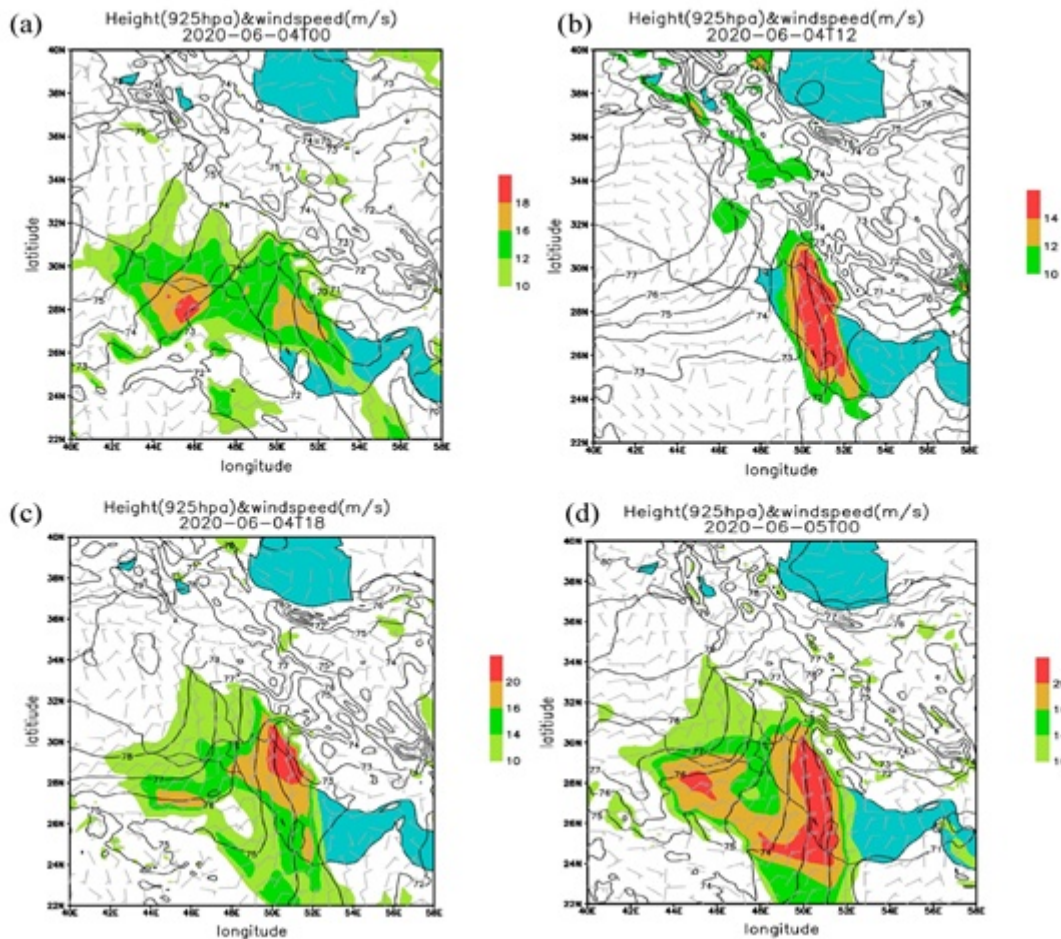


Figure3. Surface pressure and wind speed a) at 00UTC 4th Jun 2020, b) 12UTC 4th Jun 2020, c) 00UTC 5th Jun 2020, d) 12UTC 5th Jun 2020



**Figure 4.** 925-hPa Geopotential height (gpm) and wind speed ( $\text{ms}^{-1}$ ) at, a) 00UTC 4<sup>th</sup> Jun 2020, b) 12UTC 4<sup>th</sup> Jun 2020, c) 18UTC 4<sup>th</sup> Jun 2020, d) 00UTC 5<sup>th</sup> Jun 2020

These patterns in comparison with 925 hPa the wind speed was weaker on 850 hPa and extended over the smaller area.

On the 700hPa level at 18 UTC the wind speed increased to  $12 \text{ ms}^{-1}$  over north of the PG compared to past hours (Fig.6.a b).

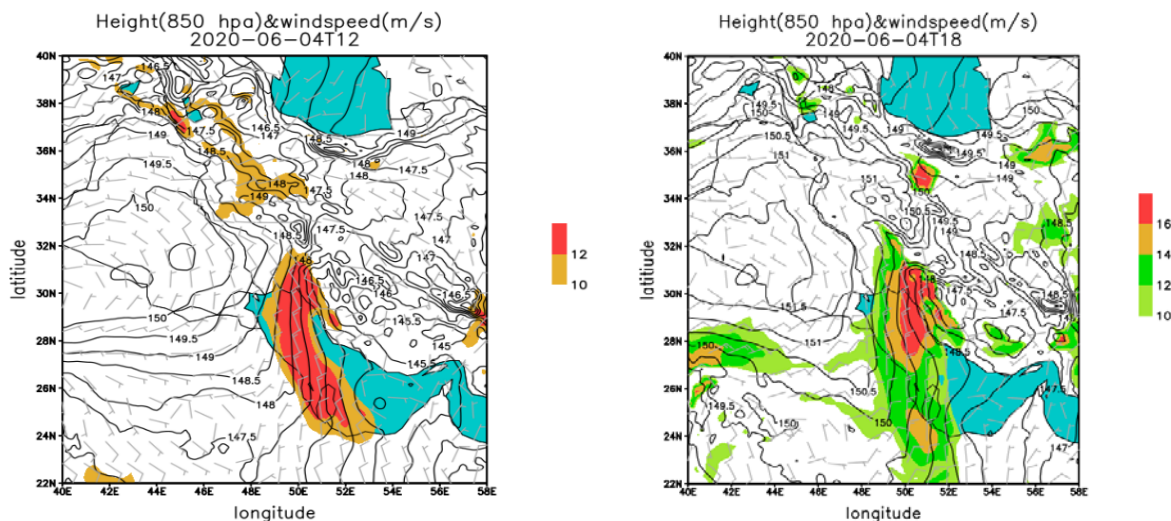


**Figure 5.** 850-hPa Geopotential height of (gpm) and wind speed( $\text{ms}^{-1}$ ) at, a) 00UTC 4<sup>th</sup> Jun 2020, b) 12UTC 4<sup>th</sup> Jun 2020, c) 18UTC 4<sup>th</sup> Jun 2020, d) 00UTC 5<sup>th</sup> Jun 2020

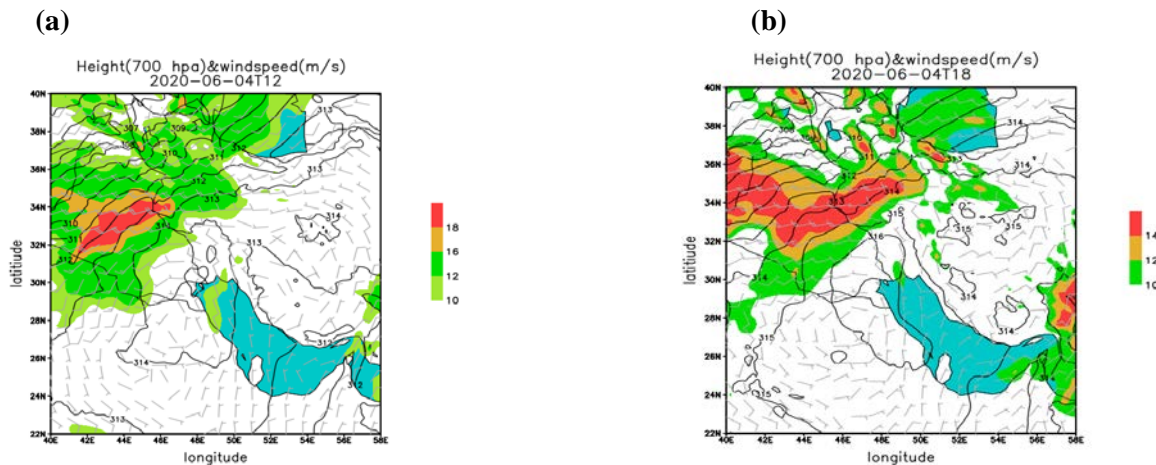


Figure 6.700- hPa Geopotential height (gpdm), wind speed ( $\text{ms}^{-1}$  ) at, a) 12UTC 4th Jun 2020, b) 18UTC 4th Jun 2020

The wind speed decreased on the 700 hPa in comparison with the lower level. From the surface to mid-troposphere, the LLJ was remarkable on the 925 hPa. There was a semi-permanent anticyclone subtropical high over Iran at mid-troposphere levels that cause the southwesterly flow over north of the PG and the western of Iran (Fig.7.a).

In the study area the wind speed at the middle level decreased to  $10 \text{ ms}^{-1}$  (Fig.7.b). There was a deep trough at upper latitudes over Turkey and North West of Iran, which accompanied by strong wind speed more than  $30 \text{ ms}^{-1}$  (Fig.7.a, b).

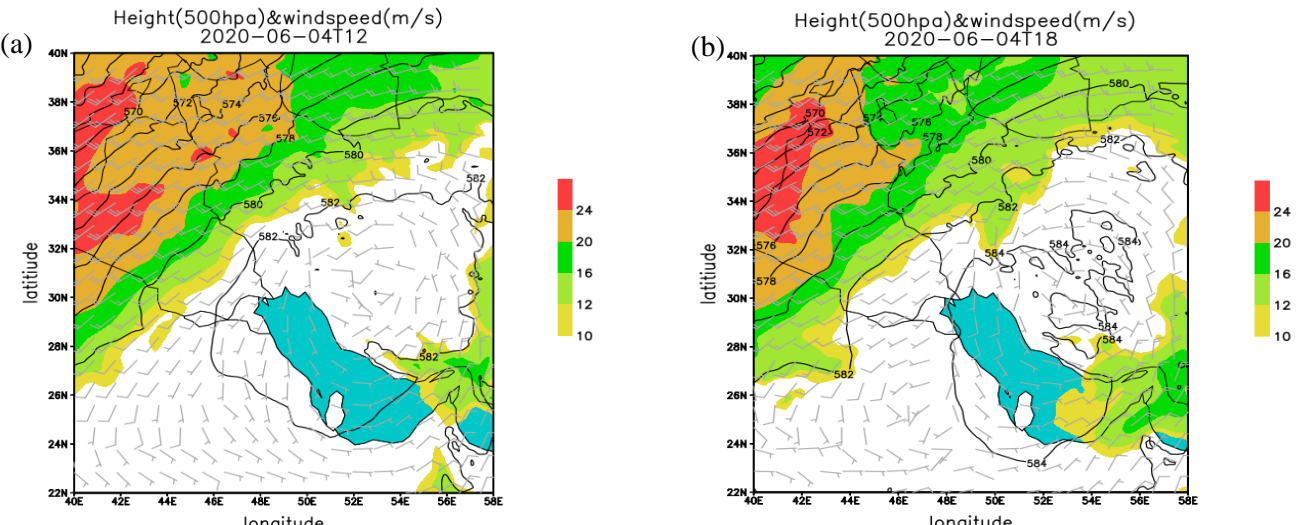


Figure 7. 500-hPa Geopotential height of (gpdm), wind speed ( $\text{ms}^{-1}$  ), a) at 12UTC 4th Jun 2020, b) 18UTC 4th Jun2020

### 3.2. Vertical wind profile

To study wind speed variations at different levels and identify the level and position of LLJ, firstly upper air data of Ahvaz, Al Qaisumeh and Aldamam (not shown here) of Saudi Arabia studied which are the nearest upper air to the Um Qasr port. Kuwait station has not recorded data during our study period so the vertical wind profile of both stations and the ports near the PG prepared. Thermodynamic instability indices such as CAPE, CIN and KI had minimal value were used to study convective phenomena on 3th to 5th Jun 2020and there was no precipitation during the study period. The value of the CAPE and CIN was zero at both stations during the study period. The KI has

increased to the maximum value of 19/9 at Al-Qaisumeh and 17 at Ahvaz station during afternoon on 4th Jun and early morning of 5th Jun. Ahvaz station has recorded data only during afternoon time (12UTC). The wind (speed and direction) shear at lower level can see very well. Figure 10 shows the wind speed at Al- Qaisumeh increased at the 900 hPa to 800 hPa level and then decreased at the levels upper than 800 hPa during afternoon on 4th Jun and 5th Jun that show the formation of LLJ. The wind direction changed backward in this shallow layer (from 900 hPa to 800 hPa), which indicates cold advection (Fig.8.d).

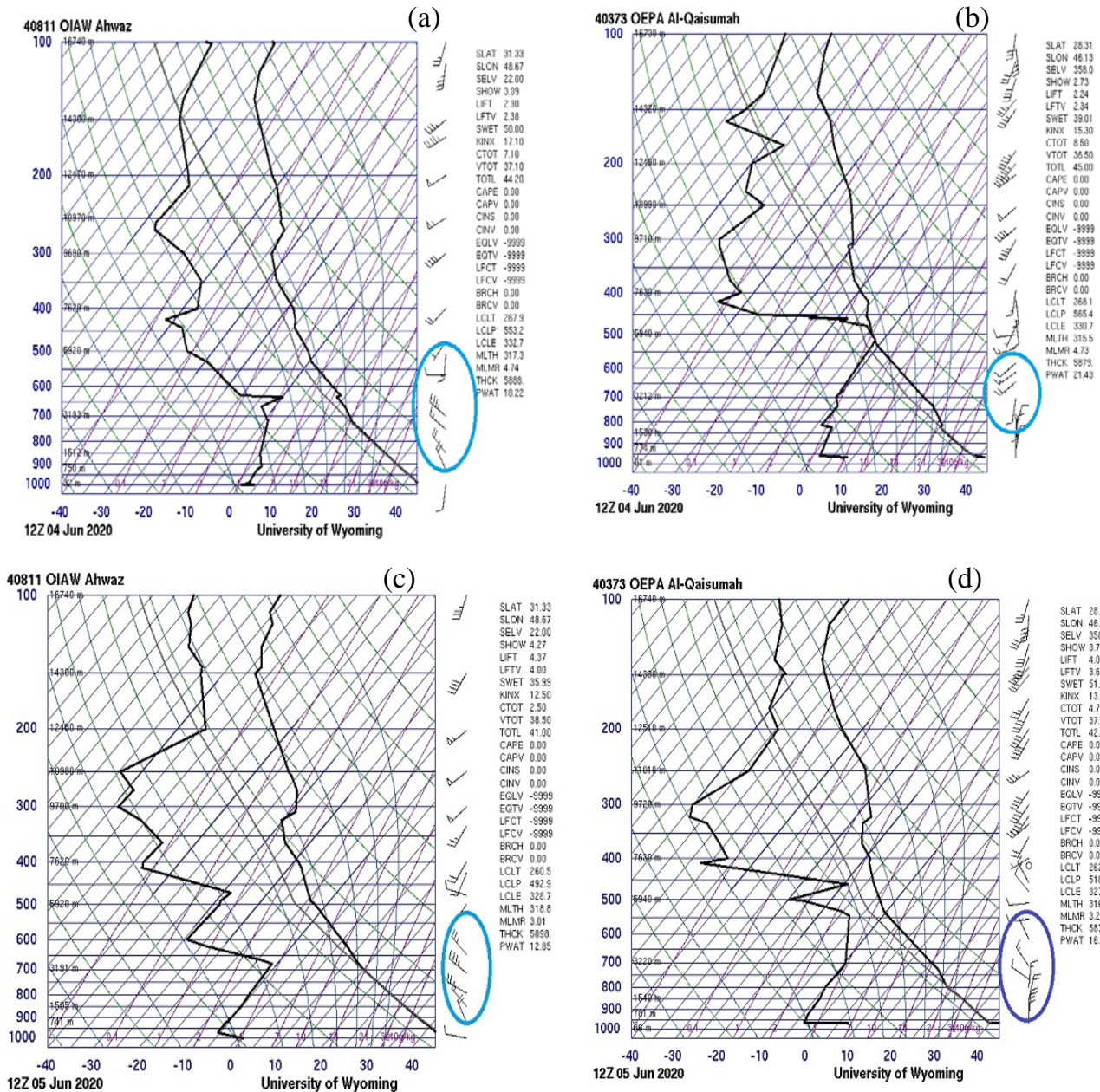
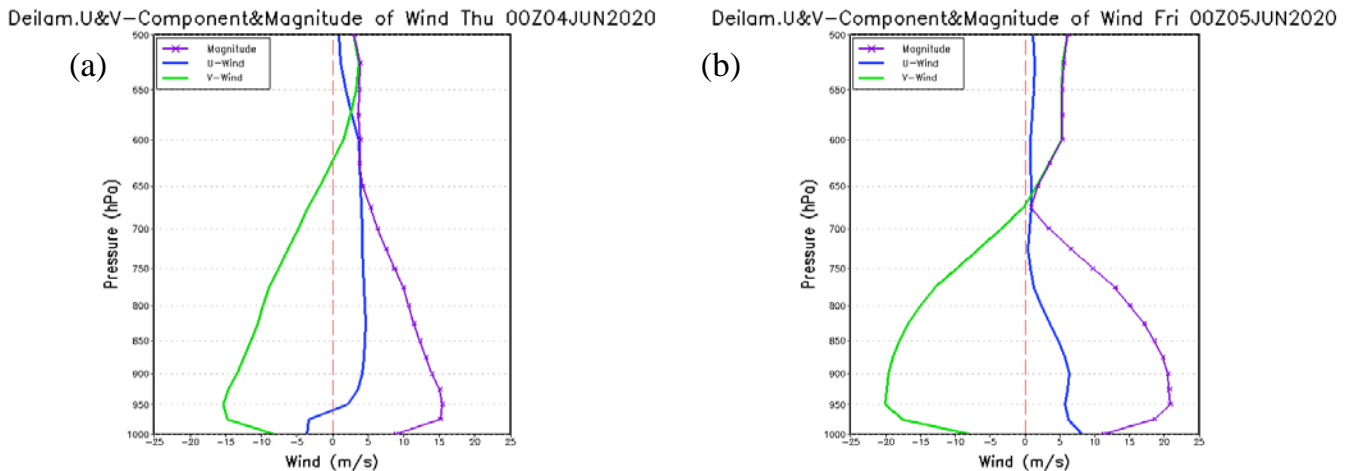


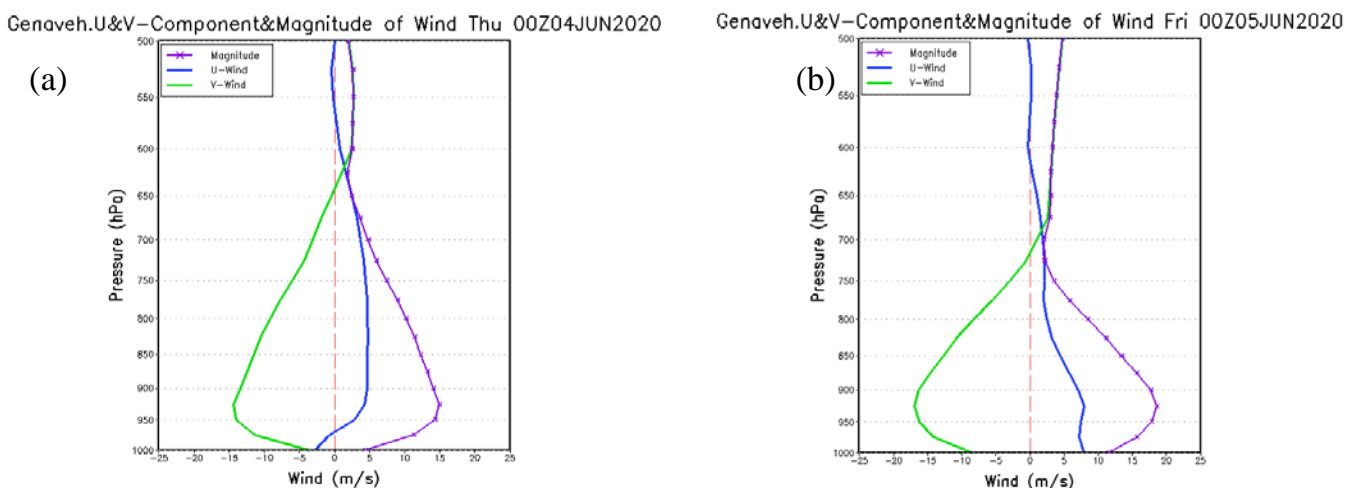
Figure 8. Skew-T diagram of a) Ahwaz and b) Al-Qaisumeh station at 12UTC 4th Jun and 12UTC 5th Jun (respectively c, d)

Figure 9 shows vertical wind profile at 00 UTC on 4th and 5th Jun over Deilam by using the WRF model output that shows LLJ at 925 hPa level. The negative values of meridional speed show northerly flow. LLJ develops at 950 hPa with more wind speed compared with the Ahwaz profile (not shown here) and the LLJ speed reached  $22 \text{ ms}^{-1}$  during early morning on 5th Jun and night of 4th Jun (18UTC).

During afternoon time on 5th Jun the wind speed decreased. At Genaveh port the LLJ exists at 925 hPa with the maximum wind speed  $20 \text{ ms}^{-1}$  (Fig.10). There is a significant difference between Kuwait wind speed profile during morning and afternoon time at the selected period. The nightly LLJ is clear at 975 hPa (Fig.11).



**Figure 9.** Deilam vertical profile of zonal wind component (blue color), meridional wind component (green color) and wind speed magnitude (purple color) at 00UTC on a) 4th Jun 2020, b) 5th Jun 2020



**Figure 10.** Genaveh vertical profile of zonal wind component (blue color), meridional wind component (green color) and wind speed magnitude (purple color) at 00UTC on a) 4th Jun 2020, b) 5th Jun 2020

The LLJ at Bushehr existed at 925 hPa level during morning time on 4th Jun and then it existed with larger

wind speed at lower level 975 hPa during afternoon and nighttime (12 and 18 UTC) (Fig.12).

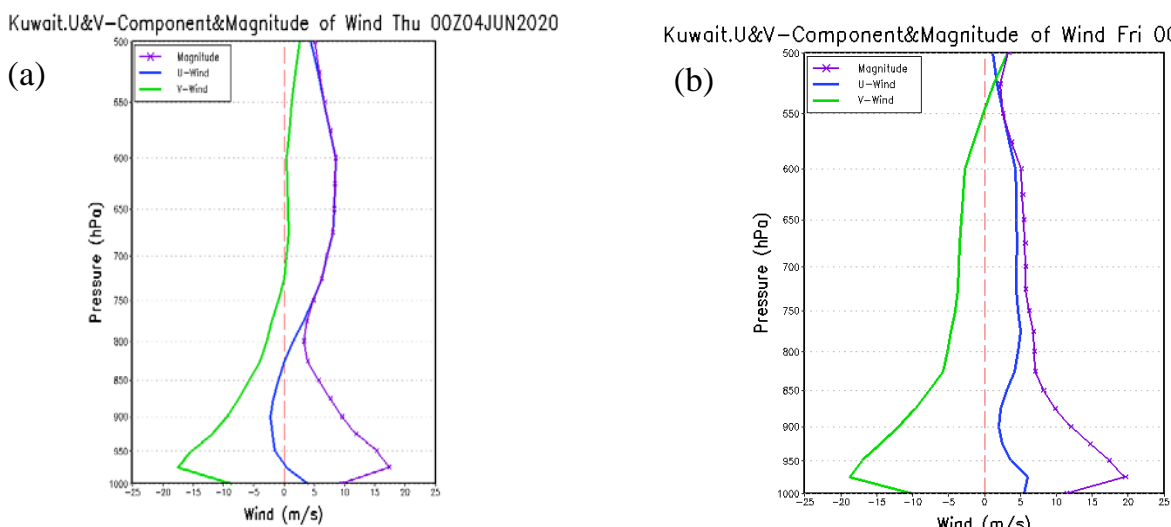


**Figure 11.** Kuwait vertical profile of zonal wind component (blue color), meridional wind component (green color) and wind speed magnitude (purple color) at 00UTC on a) 4th Jun 2020, b) 5th Jun 2020

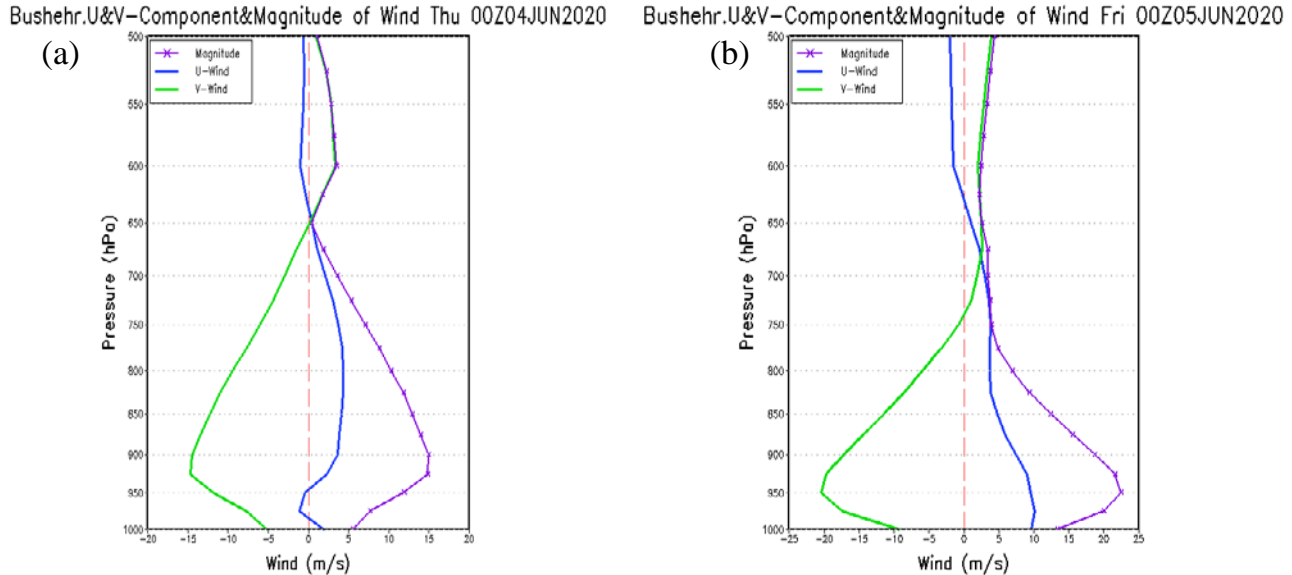


**Figure 12. Bushehr vertical profile of zonal wind component (blue color), meridional wind component (green color) and wind speed magnitude (purple color) at 00UTC on a) 4th Jun 2020, b) 5th Jun 2020**

### 3.3. Vertical cross-section of the wind speed and potential temperature

To better identify LLJ the variations in wind speed from surface to 700 hPa level by some cross sections over the study area have investigated. The first cross section crosses from Kuwait to the PG and north part of Bushehr (line AB at Fig.13). On 4th Jun 2020 (00UTC) the maximum wind speed ( $15 \text{ ms}^{-1}$ ) located over east of the PG and the minimum of the potential temperature  $34^\circ\text{C}$  is over surface and the PG (Fig.13.a). At 12 UTC on 4<sup>th</sup> Jun, increasing potential temperature have seen particularly over land because of difference between specific heat capacity of water and land. These differences between land and water's temperature and also the heat capacity are equivalent to the sensible heat flux that caused an increase in baroclinicity and is a helpful factor in increasing LLJ wind speed in the study area.

The maximum wind speed of  $17 \text{ ms}^{-1}$  can be seen over the east of PG and Bushehr from 975 hPa to 850 hPa.

The heating during day time, increasing vertical motions and increasing of the mixing layer height cause the maximum wind speed extends to the upper level (850hPa) (Fig.13.b). At 18 UTC LLJ wind speed increased to  $21 \text{ ms}^{-1}$  that was the maximum value during the past 24 hours and limited to the lower level. (From 975 hPa to 900 hPa) (Fig.13.c). There is a minimum wind speed at 850 hPa and the upper level. In the early morning on 5 Jun, LLJ, with the maximum speed of  $21 \text{ ms}^{-1}$  can be seen from the level below 950 hPa to the upper than 950 hPa (Fig.13.d). Potential temperature increased by approaching the mountain that it shows decreasing in static stability and increasing in wind speed. The second cross section is over north of Bushehr to Um Qasr and Kuwait (line CD) that shows the maximum wind speed  $15 \text{ ms}^{-1}$  during afternoon time on 4th Jun because of boundary layer turbulent mixing from 975 hPa to upper altitudes(Fig.14.a, b).

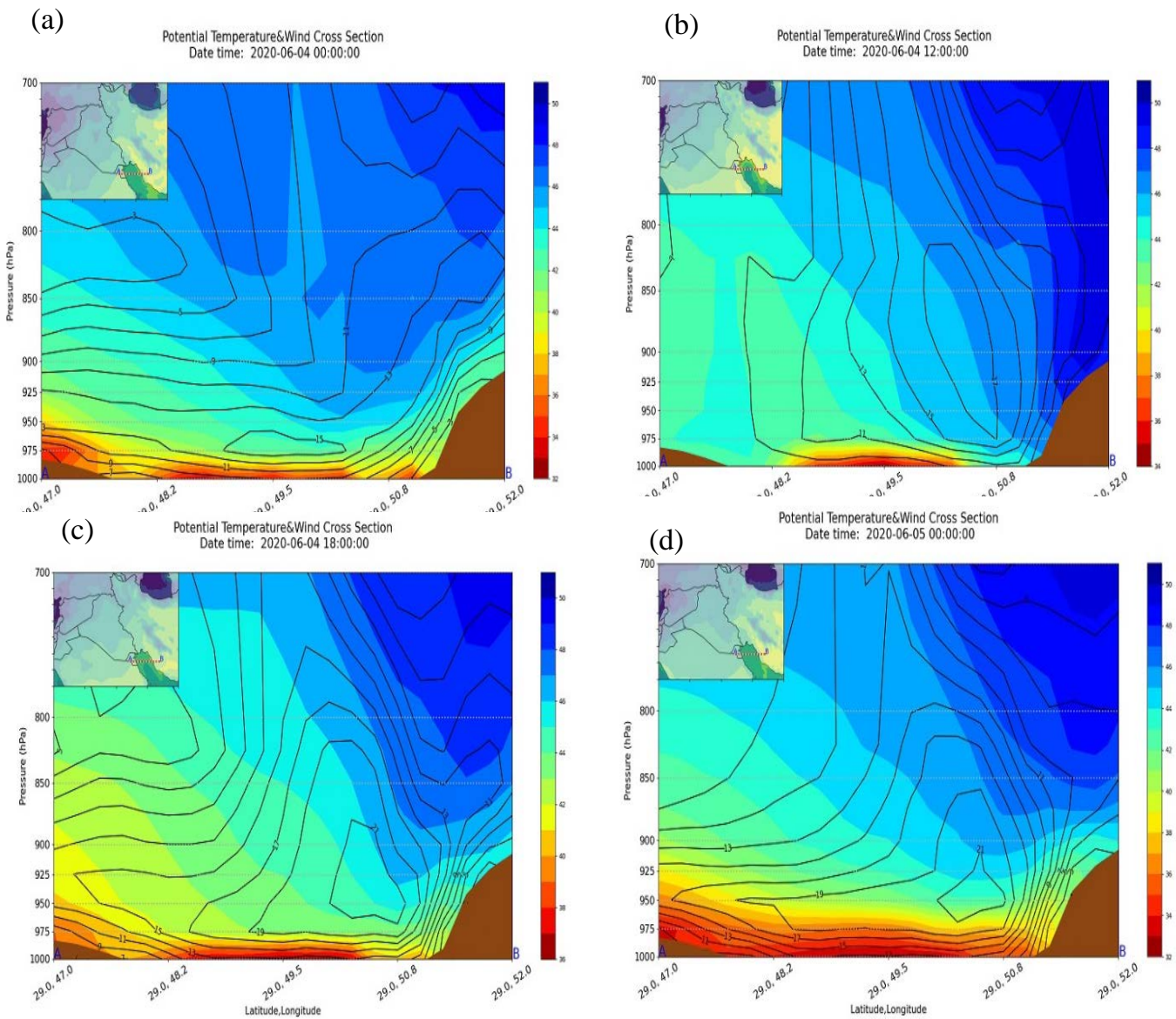


**Figure 13.** Vertical cross-sections of wind speed (black contour,  $\text{m s}^{-1}$ ) and potential temperature (shaded, C) over PG along the line from A to B from 00UTC 2020-06-04 to 00UTC on 2020-06-05(respectively a to d)

At the night of 4th Jun, the maximum speed of LLJ's core reached to  $17 \text{ ms}^{-1}$ . At early morning of 05 Jun the core speed increased to  $19 \text{ ms}^{-1}$  and cover larger area but only around 950 hPa (Fig.14.c, d). Adiabatic changes in temperature cause decreasing in potential temperature during nighttime of 4th Jun and early morning of 5th Jun (Fig.14.c, d). As discussed at synoptic patterns, the pressure systems caused northerly flow over southwest of Iran and PG that

figure 15 shows the vertical diagrams over some places near to Um Qasr (the position which Behbahan cargo vessel sank) such as Deilam port and Abadan, Bushehr, Genaveh port, Khorramshahr, Kuwait are not shown here (Fig.15).

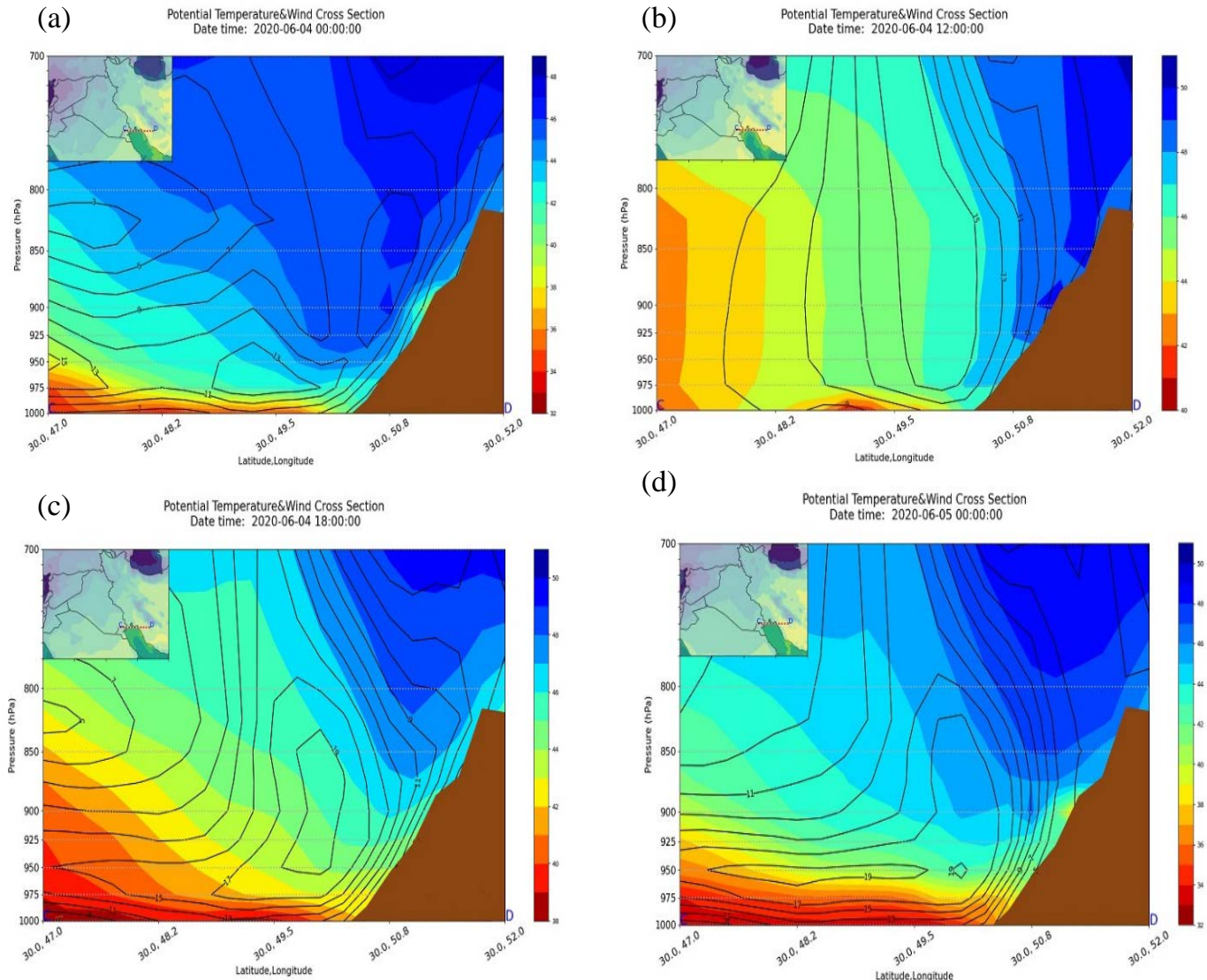


**Figure 14.** Vertical cross-sections of wind speed (black contour,  $\text{m s}^{-1}$ ) and potential temperature (shaded, C) over PG along the line from C to D from 00UTC 2020-06-04 to 00UTC on 2020-06-05(respectively a to d)

These diagrams show the formation of LLJ by the maximum wind speed  $25\text{ms}^{-1}$  from 975 hPa level to 950 hPa and then decreasing at upper levels. The maximum wind speed of the LLJ formed over northern part of the PG such as Bushehr and Genaveh port. By using model output data, the vertical profile of wind speed and the time of formation of LLJ (night of 4th Jun and early morning of 5th Jun with the maximum

speed  $18 \text{ ms}^{-1}$  at 950 hPa level) over Kuwait and Abadan shown. The other diagrams also show the same time for the LLJ formation. (Fig.16). LLJ formed at lower level at Kuwait, Bushehr, Abadan and Ahvaz but at Deilam port and Genaveh port LLJ formed at the level upper than 950 hPa near to the 850 hPa (Fig.16).

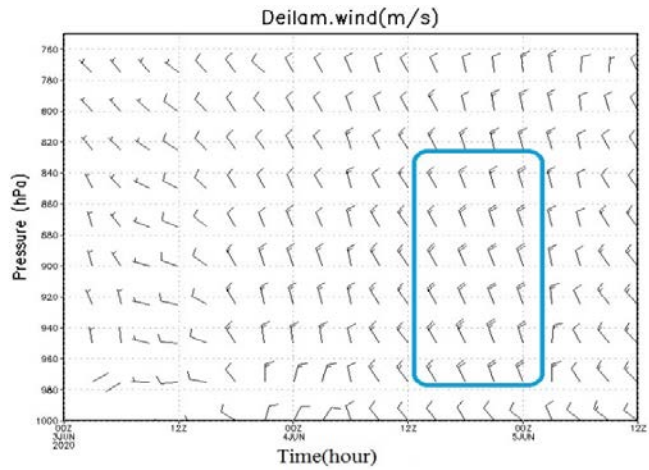
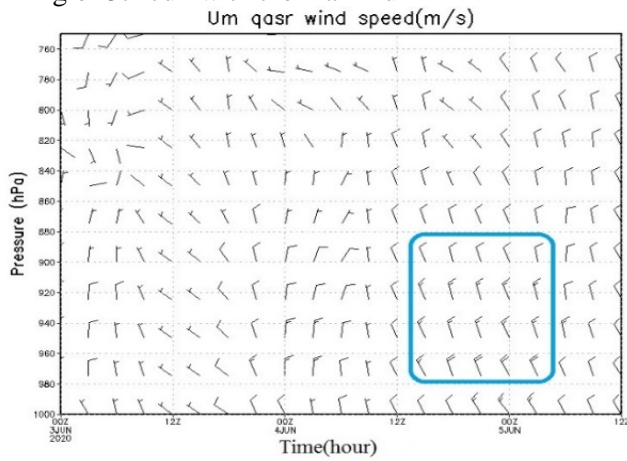


**Figure 15.** Vertical profile of wind speed ( $\text{m s}^{-1}$ ) over some points of the study area from 2020-06-03 to 12UTC of 2020-06-05

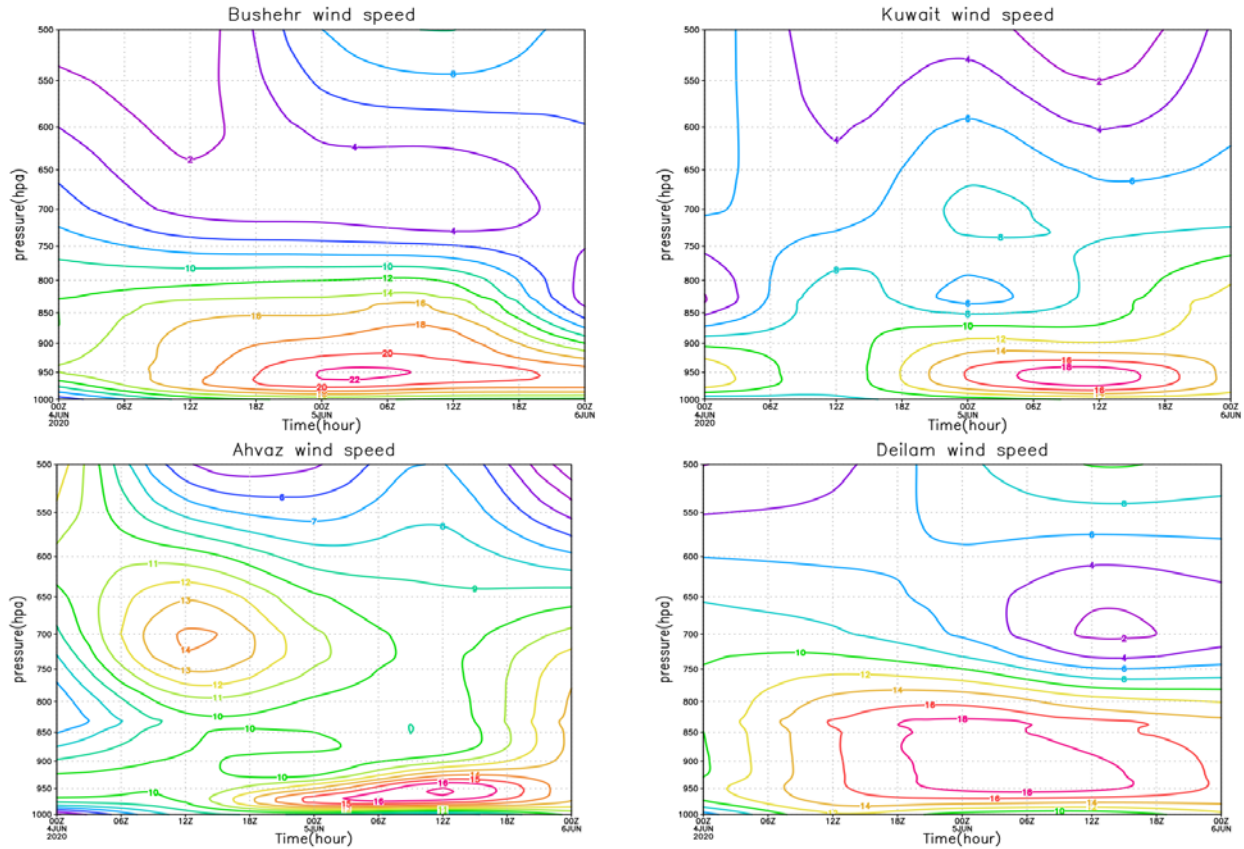


Figure 16. Time cross section of wind speed ( $\text{m s}^{-1}$ ) over some points of our study area from 2020-06-03 to 12UTC of 2020-06-05

#### 4. Conclusions

Mesoscale LLJs over southwest of Iran and Northern the PG (NPG) are essential in rippling NPG and shipping. Throughout the nighttime in the warm season, because of cooling and decreasing turbulent mixing layer's height, the decoupling of surface layer from boundary layer occurs, which reduces friction and increases the wind speed at upper level than surface layer. At surface pressure pattern, there is a high system over the Zagros mountain area that increases to its maximum 1016 hPa during LLJ formation time. A low pressure system 1004 hPa forms simultaneously over south of the PG that a deep surface trough extends northward to the north of the PG and Khuzestan that causes an increasing in the east- west pressure gradient. At 925 hPa, the pattern looks like to the surface map and there is a low system over the PG that its trough extends to the north of the PG. A high system forms east of the Mediterranean Sea that its ridge extends to the west of Iran and then gradually extends to the east and the trough extends to higher latitudes that simultaneously increased pressure gradient over the study area and increased wind speed from nighttime of 4th Jun to 5th Jun. At 850 hPa the pattern is similar to the 925 hPa level, but by less instability which geopotential gradient is weak so the wind speed is also weak. At the upper levels the instabilities going weaker so the best level at which the LLJ formed was 925 hPa. Ahvaz's Skew-T diagrams (12UTC) showed northwesterly winds with an intense speed at the lower

than 700 hPa level. The LLJ can be seen at 925 hPa at Al-Qaisumah and Al-damam port. The instability indexes like CIN, CAPE, were very low. The KI has had a little increase during nighttime of 4th Jun and morning of 5th Jun. The study of anomaly of surface wind speed shows increasing anomaly during the time of the LLJ formation that the maximum value  $6 \text{ ms}^{-1}$  was on 5th Jun morning. LLJ has formed mostly at altitudes from 975 to 950 hPa. The maximum wind speed of the LLJ was over Bushehr shores especially Bushehr and Genaveh  $22 \text{ ms}^{-1}$  and  $20 \text{ ms}^{-1}$  respectively during nighttime (18 UTC) 4th Jun and 5th Jun morning (00UTC). The cross section of wind speed and potential temperature show increasing of wind speed during the LLJ formation's time that because of the weakness of the turbulent mixing the increasing of wind speed happens at the lower levels while during morning and afternoon time the turbulent mixing increases and the wind speed decreases. Time cross sections showed that the LLJ at some regions like Kuwait, Bushehr and Abadan formed at lower heights (under 950 hPa) and at the other points formed at upper levels (950 hPa to 850 hPa) but LLJ in the study area formed during nighttime of 4th Jun to afternoon of 5th Jun 2020. Due to the low height of LLJs, the momentum transmit to the surface quickly, significantly during morning time which causes increasing the surface wind speed, the wave height over the PG and the disturbances in vessels and boats movement. Temperature differences and specific heat

capacity difference between land and sea over the PG are the other factors that cause baroclinicity and form the LLJ. Behbahan vessel sank during the early morning of 5th Jun because of the formation of LLJ.

## Acknowledgment

We are appreciative of helps and very valuable comments of Mr. Mostafa Hadizadeh (North Khorasan Meteorological Administration).

## 5. References

- 1- Bonner, W. D., (1968), *Climatology of the low level jet*. Mon. Wea.Rev., Vol. 96, pp.833–850.
- 2- Doyle, J. D., Warner, T. T., (1993), *A three-dimensional numerical investigation of a Carolina coastal low-level jet during GALE IOP*. Mon Wea Rev, Vol. 121(4), pp.1030–1047.
- 3- Whiteman, C. D., Bian, X., Zhong, S., (1997), *Low-level jet climatology from enhanced rawinsonde observations at a site in the Southern Great Plains*. J Appl Meteor, Vol. 36(10), pp.1363–1376.
- 4- Colle, B. A., Novak, D. R., (2010), *The New York Bight jet: climatology and dynamical evolution*. Mon Wea Rev, Vol. 138(6), pp.2385–2404.
- 5- Rife, D. L., Pinto, J. O., Monaghan, A. J., Davis, C. A and Hannan, J. R., (2010), *Global distribution and characteristics of diurnally varying low-level jets*. J Clim, Vol. 23(19), pp.5041–5064.
- 6- Hu, X. M., Klein, P. M., Xue, M., Lundquist, J. K., Zhang, F. and Qi, Y., (2013), *Impact of low-level jets on the nocturnal urban heat island intensity in Oklahoma City*. J Appl Meteorol Climatol, Vol.52 (8), pp.1779–1802.
- 7- Berg, L. K., Riihimaki, L. D., Qian, Y., Yan, H. and Huang, M., (2015), *The low level jet over the Southern Great Plains determined from observations and reanalyses and its impact on moisture transport*. J Clim, Vol. 28(17), pp.6682–6706.
- 8- Vanderwende, B. J., Lundquist, J. K., Rhodes, M. E., Takle, E. S. and Irvin, S. L., (2015), *Observing and simulating the summertime low-level jet in central Iowa*. Mon Wea Rev, Vol. 143(6), pp.2319–2336.
- 9- Smith, E. N., Gebauer, J. G., Klein, P. M., Fedorovich, E and Gibbs, J. A., (2019), *The Great Plains low-level jet during pecan: observed and simulated characteristics*. Mon Wea Rev, Vol.147 (6), pp.1845–1869.
- 10- Blackadar, A. K., (1957), *Boundary layer wind maxima and their significance for the growth of nocturnal inversions*. Bulletin of the American Meteorological Society, Vol.38, PP. 283–290.
- 11- Holton, J.R., (1967), *The diurnal boundary-layer wind oscillation above sloping terrain*. Tellus,Vol 19, pp. 199–205.
- 12- Bonner, W.D., Paegle, J., (1970), *Diurnal variations in boundary-layer winds over the south-central United States in summer*. Mon. Weather Rev, Vol. 98, pp. 735–744.
- 13- Markowski, P and Richardson, Y., (2011), *Mesoscale meteorology in midlatitudes*, Wiley-Blackwell, ISBN: 978-0470742136. 430 pp.
- 14- Membery, D.A., (1983), *Low-level wind profiles during the Gulf Shamal*. Weather, Vol. 38, pp. 18–24.
- 15- Rao, P. G., Hatwar, H. R., Al-Sulaiti, M. H and Al-Mulla, A. H., (2003), *Summer Shamals over the Arabian Gulf*. Weather, Vol. 58, pp. 471–478.
- 16- Stull, R. B., 1988. *An Introduction to Boundary Layer Meteorology*. Kluwer Academic, 670 pp.
- 17- Liu, M., Westphal, D. L., Holt T. R. and Xu, Q., (2000), *Numerical simulation of a low-level jet over complex terrain in southern Iran*. Monthly Weather Review, Vol.128, pp. 1309–1327.
- 18- Alizadeh-Choobari, O., Zawar-Reza, P. and Sturman, A., (2014), *The wind of 120 days and dust storm activity over the Sistan Basin*. Atmospheric Research, Vol 143, pp. 328 –341.
- 19- Gevorgyan, A., (2018), *A Case Study of Low-Level Jets in Yerevan Simulated by the WRF Model*. Journal of Geophysical Research: Atmospheres, Vol.123, pp.300–314.
- 20- Vazifeh, A., Aliakbari-Bidokhti, A. A., Mazraeh Farahani, M., (2019), *A climatological study of the Low Level Jet in Central Desert of Iran (Dashte Kavir)*. Journal of the Earth and Space Physics, Vol. 45(3), pp. 687-704.
- 21- Bidokhti, A. A., Boromand, N., (2006), *Study of Gap Winds in the Lut Plateau*. Desert, Vol.11 (1), pp.13-30.
- 22- Mobarak Hass, E., Ghafarian, p., (2018), *Low- level Jet (LLJ) Simulation by Different WRF- Chem Boundary Layer Schema in Khuzestan province*. J. Meteorol. Atmos. Sci., vol 1(2), pp.287-303.
- 23- Giannakopoulou, E. M. and Toumi, R., (2012), *The PG summertime low-level jet over sloping terrain*. Q. J. R. Meteorol. Soc, Vol. 138, pp.145–157.
- 24- Du, Y., Chen, Y. L., Zhang, Q., (2015), *Numerical simulations of the boundary layer jet off the southeastern coast of China*. Mon Wea Rev, Vol.143 (4), pp.1212–1231.
- 25- Chen, F., & Dudhia, J., (2001), *Coupling an advanced land-surface/hydrology model with the Penn State/NCAR MM5 modeling system. Part I: Model description and implementation*. Monthly Weather Review, vol. 129(4), pp.569– 585.
- 26- Dudhia, J., (1989), *Numerical study of convection observed during the Winter Monsoon Experiment using a mesoscale two dimensional model*. Journal of the Atmospheric Sciences, vol. 46(20), pp.3077– 3107.
- 27- Mlawer, E. J., Taubman, S. J., Brown, P. D., Iacono, M. J. and Clough, S. A., (1997), *Radiative transfer for inhomogeneous atmosphere: RRTM, a validated correlated-k model for the long-wave*. Journal of Geophysical Research, vol. 120, pp.663– 682.